minerals

MDPI

Article

Adsorption and Desorption of Coal Gangue toward Available Phosphorus through Calcium-Modification with Different pH

Tiantian Ye [1], Xiangyu Min [1,2,*], Xuzi Jiang [1], Mingyue Sun [1] and Xinju Li [1,2]

[1] College of Resources and Environment, Shandong Agricultural University, Taian 271018, China; 2020110355@sdau.edu.cn (T.Y.); 2020110362@sdau.edu.cn (X.J.); 2020120469@sdau.edu.cn (M.S.); lxj0911@126.com (X.L.)

[2] National Engineering Research Center for Efficient Utilization of Soil and Fertilizer Resources, Taian 271018, China

* Correspondence: minxy1991@sdau.edu.cn

Abstract: The chemical reaction between calcium ions (Ca^{2+}) and phosphate in the soil is the main way to maintain the availability of soil phosphorus. Thus, we believe stimulating coal gangue with Ca^{2+} solution would be an effective way to improve its adsorption and desorption capacity toward phosphate. In order to explore the effects of different pH of Ca^{2+} solution on the modified effect of coal gangue, we conducted mechanical grinding (<1 mm), high temperature calcination (800 °C), and the stimulation of Ca^{2+} solution with different pH (2, 7, 13), to prepare acidic calcium-modified coal gangue (Ac-CG) (Ac-CG, acidic calcium-modified coal gangue; Ne-CG, neutral calcium-modified coal gangue; Al-CG, alkali calcium-modified coal gangue; RCG, raw coal gangue), neutral calcium-modified coal gangue (Ne-CG), and alkali calcium-modified coal gangue (Al-CG); raw coal gangue (RCG) was regarded as the control. The results indicated that Al-CG had better phosphate adsorption (3.599 mg g^{-1}); this favorable adsorption performance of Al-CG was related to the formation of hydrated calcium silicate gel and ettringite, which provided more Ca^{2+}, Al^{3+}, and hydroxyl groups, and a larger specific surface area (9.497 m^2 g^{-1}). Moreover, Al-CG not only held more phosphate but also maintained its availability longer for plants. It is suggested that stimulating coal gangue with Ca^{2+} solution under alkaline conditions is a perfect way to enhance its adsorption and desorption capacity toward phosphate; the Al-CG we prepared could be used as filling material and soil conditioner in the reclamation area.

Keywords: calcium-modified coal gangue; available phosphate; reclaimed minesoil; adsorption and desorption

Citation: Ye, T.; Min, X.; Jiang, X.; Sun, M.; Li, X. Adsorption and Desorption of Coal Gangue toward Available Phosphorus through Calcium-Modification with Different pH. *Minerals* **2022**, *12*, 801. https://doi.org/10.3390/min12070801

Academic Editor: María Ángeles Martín-Lara

Received: 23 May 2022
Accepted: 22 June 2022
Published: 24 June 2022

1. Introduction

Coal gangue is the main solid waste generated during coal mining and washing, accounting for about 10–25% of total coal production [1–4]. With the progress of coal mining activities, coal gangue accumulates in large quantities; it has become one of the largest industrial residues [5,6]. The accumulation of coal gangue not only occupies large land resources but also causes serious environmental problems, such as soil pollution, soil degradation, geological disasters, and air pollution [7–16]. Therefore, it is an urgent international task to improve the comprehensive utilization efficiency of coal gangue and eliminate its negative impact on the ecological environment [17].

Coal mining causes massive land destruction, which is exhibited by the subsidence of surface morphology and the rising of the groundwater [18–20], and reclamation is regarded as the critical method to restore the subsidence land. Moreover, coal gangue has large storage capacity and is used as the common alternative soil substrate to filling the coal mining subsidence area [21–23], which not only reduces the land occupation but also realizes waste reuse [21]. However, some scholars reported that the filling of coal gangue is not conducive to nutrient sequestration: the soil nutrients are lost rapidly

after passing through the coal gangue filling layer, resulting in in low nutrient content of reclaimed soil [9,24]. In addition, the primary utilization of coal gangue inevitably causes secondary environmental pollution such as water eutrophication [21]. Therefore, improving the retention capacity of coal gangue toward soil nutrient elements is significant in the reclamation of coal mining area. Thus, it can be seen that increasing the retention capacity of coal gangue to nutrients is of great significance to improve the application of coal gangue as an alternative soil substrate the in coal mining subsidence area.

The main components of coal gangue are SiO_2 and Al_2O_3, accounting for 60–95%, and the its chemical structure is stable, with limited adsorption capacity for chemical elements [8,25,26]. However, it is rich in porous structures and clay minerals and is used as adsorbent or adsorbent feedstock by related scholars, and mechanical grinding, thermal activation, and chemical activation are common methods to enhance the reactivity of coal gangue [10,27–32]. Mechanical activation is a physical change of coal gangue by grinding processes. Grinding transformed the crystal structure, changed the crystalline degree, and increased the active reaction site of coal gangue and therefore enhanced the reaction activity of coal gangue [33–35]. The thermal activation is an effective method to stimulate the activity of coal gangue. The generated amorphous reactive SiO_2 and Al_2O_3 after thermal activation improved the reactivity of coal gangue [36–38]. Chemical activation is a method of causing chemical agents to react with amorphous aluminosilicates, which produces inorganic binders with chemical and physical properties. Han et al. [39] prepared coal gangue–slag composite materials with sodium silicate as an activator; some scholars have also improved the reactivity of coal gangue by acid leaching [40,41]. Although the above literature has proved that activation can enhance the adsorption performance of gangue, few studies have reported the effect of activated gangue on the adsorption and desorption capacity of nutrient ions; especially, whether the adsorbed nutrients can be effectively released is still unknown, which affects the application of gangue in agricultural production. Phosphorus is one of the main soil-nutrient elements; even though related scholars have prepared lanthanum-modified and sodium-modified coal gangue to remove phosphate from water [42], the adsorption of phosphate with those modified methods is irreversible, which affects their application in agricultural production. It is well known that combining soil phosphate with calcium ion (Ca^{2+}) to form calcium phosphate salts is the main method of soil phosphorus retention, and calcium addition benefits the sequestering of soil active phosphorus and the maintaining of its effectiveness for plants [43]; thus, we believe activating coal gangue with Ca^{2+} would increase its adsorption and desorption capacity toward phosphorus. Currently, few works have been completed so far to study modified coal gangue with calcium to adsorb phosphorus; especially, the effect of the pH of calcium solutions on the adsorption and desorption characteristics has remained unclear now, so this study will fill the gap of related studies.

Here, we prepared three different calcium-modified coal gangues through grinding, calcination, and stimulating, with $CaCl_2$ solutions with different pH, to explore the effect of $CaCl_2$ solutions pH on the adsorption and desorption capacity of modified coal gangues toward phosphate and its mechanism. Therefore, (i) the structure, morphology, composition, and porosity of the raw and calcium-modified coal gangues were systematically characterized; and (ii) their adsorption and desorption characteristics toward phosphate were systematically studied. This study further improved the activation method of coal gangue and broadened the application scope of activated coal gangue, and these results are expected to improve the utilization of coal gangue in agriculture and reclamation in coal mining area.

2. Materials and Methods

2.1. Material Collection and Preparation

The coal gangue used in this study was collected from Yanzhou mine area in Jining city, Shandong province. After removing impurities, the samples were crushed and sieved by 1 mm sieve to get raw coal gangue (RCG). The RCG with muffle furnace (Nabertherm

LT15/12, Lilienthal, Germany) were calcined in 800 °C for 2 h and cooled to room temperature, and then the samples were reacted with $CaCl_2$ solutions with a solid–liquid ratio of 0.12 and a reacting temperature of 98 °C for 4 h at different pH conditions (2, 7, and 13), which were adjusted with HCl and NaOH solutions. After that, the samples were rinsed to neutral with distilled water and air-dried to obtain acidic calcium-modified coal gangue (Ac-CG), neutral calcium-modified coal gangue (Ne-CG), and alkaline calcium-modified coal gangue (Al-CG).

2.2. Characterization

Evaluated in conjunction with the detailed clay mineral analysis of the <2 μm fraction of raw and modified samples by oriented-aggregate X-ray diffraction methods (XRD, Bruker D8 ADVANCE, Karlsruhe, Germany), the contents of elemental components were measured by X-ray fluorescence spectrometer (XRF, PANalytical Axios, Amsterdam, Netherlands). The distribution of functional groups was measured by Fourier transform infrared spectroscope (FTIR, Nicolet iS50, New York, USA). The structural morphology of the sample surface was observed by scanning electron microscope (SEM, Zeiss Sigma 300, Oberkochen, Germany). The specific surface area and pore structure were measured based on the multipoint Brunauer–Emmett–Teller (BET, Micromeritics Gemini 2.0, Norcross, GA, USA) method.

2.3. Adsorption Experiments

2.3.1. Adsorption Kinetic Experiments

In this study, KH_2PO_4 solution (AR, KCRC, Tianjin, China) was used to simulate soil-available phosphorus; 300 mg/L KH_2PO_4 solution was prepared, and 1 g each of RCG, Al-CG, Ne-CG, and Ac-CG was weighed and put into 50 mL centrifuge. We added 25mL KH_2PO_4 solution (pH = 6.0) in the centrifuge tubes, which were shaken by oscillator (220 rpm/min, Ronghua KS, Shanghai, China) for different times (0.5, 2.5, 5, 7.5, 10, 20, 30, and 40 h); after that, we filtered the mixture with 0.45 μm aqueous filters and measured the phosphate concentration of the filtrates using a UV-Vis spectrophotometer (UV-5500, Shanghai, China). The phosphate adsorption capacities were described by the adsorption kinetic model and calculated using Equations (1) and (2):

$$\text{Pseudo first} - \text{order model } q_t = q_e\left(1 - e^{-k_1 t}\right) \quad (1)$$

$$\text{Pseudo second} - \text{order model } q_t = k_2 q_e^2 t/(1 + k_2 q_e t) \quad (2)$$

where q_e and q_t correspond to phosphate adsorption capacity at equilibrium time and at time t, respectively. k_1 and k_2 correspond to model-specific rate constants.

2.3.2. Adsorption Isotherm Experiments

KH_2PO_4 solutions of different concentrations (10, 20, 50, 100, 150, 200, 250, and 300 mg L^{-1}) were configured separately; 1 g samples of RCG, Ac-CG, Ne-CG, and Al-CG were weighed and put into 50 mL centrifuge tubes with 25 mL KH_2PO_4 solutions (pH = 6.0) with different concentrations and shaken by oscillator at 220 r/min for 24 h. The mixture was filtered through 0.45 μm aqueous filter, and the phosphate content in the filtrate was determined using the UV-Vis spectrophotometer. The phosphate adsorption capacities were described by the isotherm adsorption model and calculated using Equations (3) and (4):

$$\text{Langmuir isotherm model } q_e = K_l q_m C_e/(1 + K_l C_e) \quad (3)$$

$$\text{Freundlich isotherm model } q_e = K_f C_e^{1/n} \quad (4)$$

where k_l and k_f are the Langmuir and Freundlich constants, respectively; q_m denotes the Langmuir maximum adsorption capacity; C_e represents the equilibrium solution concentration; and n is the Freundlich linearity constant.

2.4. Desorption Experiments

The samples after the adsorption isotherm experiment were collected, air-dried, and desorbed with distilled water (pH = 7) and 0.5 mol/L $NaHCO_3$ solutions (pH = 8.5, AR, KCRC, Tianjin, China) for 10 h, respectively. $NaHCO_3$ solution can effectively extract phosphate and is a common solution for extracting soil available phosphorus; thus, we selected it as desorbent to measure the availability of the adsorbed phosphorus of the samples. Then, we collected the filters through 0.45 μm aqueous filter and measured their phosphate concentrations. Moreover, the samples after 40 h of adsorption in the adsorption kinetics experiment were also collected, air-dried, and desorbed with two desorbents for different times (0.5, 2, 4, 6, 8, and 10 h), and the phosphate concentration of the filter was measured.

2.5. Statistical Analysis

The measured data are expressed as the mean value of triplicate experiments. All data were analyzed by one-way variance (ANOVA) using SPSS 19.0 software (SPSS Inc., Chicago, IL, USA), and images were drawn using Origin 2021 software (Origin Lab., Northampton, MA, USA).

3. Results

3.1. Characterization of Raw and Calcium-Modified Coal Gangues

3.1.1. XRD Analysis

XRD patterns of RCG and modified coal gangue samples are presented in Figure 1a. As shown in the XRD patterns, the dominant mineral phases of RCG were quartz (SiO_2), kaolinite ($Al_2(Si_2O_5)(OH)_4$), and illite ($KAl_2[(OH)_2AlSi_3O_{10}]$), while the characteristic diffraction peaks of kaolinite and illite completely disappeared in the patterns of calcium-modified coal gangues. This may have been due to the hydroxyl (-OH) removal process during grinding, and high temperature calcination [44–46], where kaolinite is transformed to metakaolinite, and metakaolinite and illite are further decomposed into amorphous SiO_2 and Al_2O_3 [47]. Moreover, new phases were observed in the XRD pattern of Al-CG, which were the calcium silicate hydrate (C-S-H gel) phase and the ettringite phase (AFt); the appearance of C-S-H was attributed to a hydration reaction among SiO_2, Al_2O_3, and Ca^{2+}, and the AFt was associated with the reaction of $[Al(OH)_6]^{3-}$, Ca^{2+}, and sulphate (SO_4^{2-}).

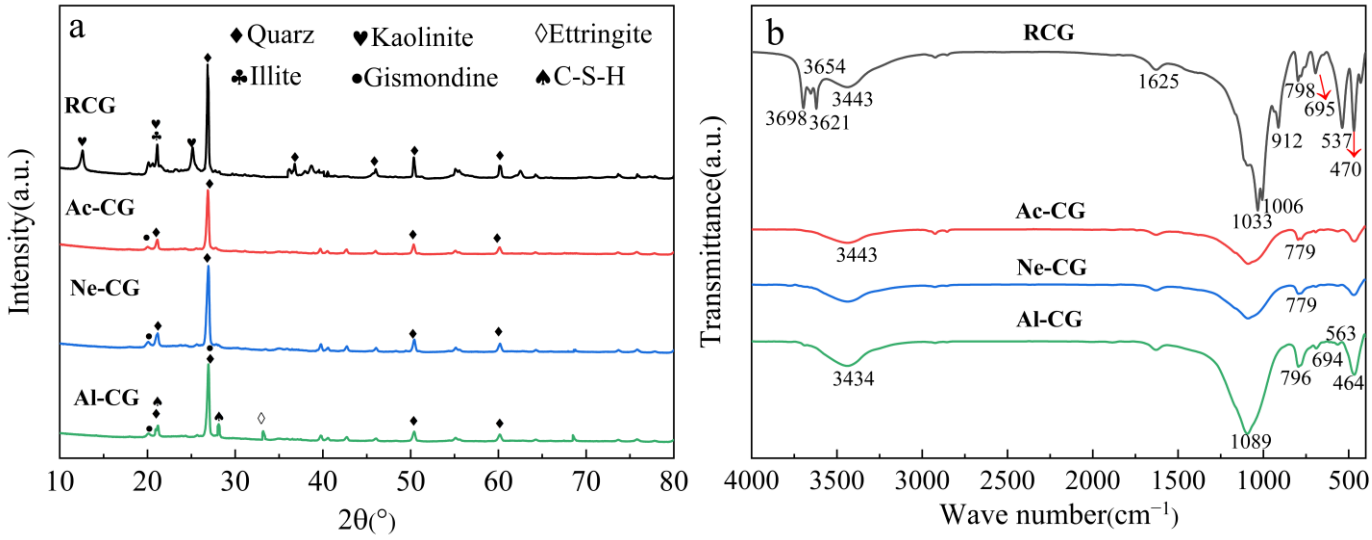

Figure 1. XRD patterns (**a**) and FTIR curves (**b**) of coal gangue samples.

3.1.2. XRF Analysis

The chemical components in RCG and calcium-modified coal gangues were shown in Table 1; these elements were represented by oxides forms. It can be seen that the major

constituents in the RCG sample were SiO_2 (64.414%), Al_2O_3 (26.468%), Fe_2O_3 (3.576%), and K_2O (2.269%), and minor constituents contained CaO, P_2O_5, SO_3, and MgO. After modification, the content of major chemical components rarely changed, while CaO and SO_3 in minor components changed noticeably. CaO increased from 1.051% in RCG to 1.179% in Ac-CG, and from 1.307% in Ne-CG to 1.628% in Al-CG, respectively, while SO_3 decreased from 1.570% in RCG to 0.775% in Ac-CG, 0.605% in Ne-CG, and 0.569% in Al-CG, indicating that SO_4^{2-} in RCG was released into solution after modification and reacted with Ca^{2+} to form new phases.

Table 1. Physiochemical properties of coal gangue samples.

Sample ID	Elemental Composition (Weight%)								Surface Area ($m^2 \cdot g^{-1}$)		Pore Volume ($cm^3 \cdot g^{-1}$)		Pore Diameter (nm)
	SiO_2	Al_2O_3	Fe_2O_3	K_2O	CaO	P_2O_5	SO_3	MgO	S_{BET}	$A_{t\text{-}Plot}$	V_{meso}	$V_{t\text{-}Plot}$	D_{avr}
RCG	64.414 ± 0.24	26.468 ± 0.22	3.576 ± 0.11	2.269 ± 0.08	1.051 ± 0.05	0.150 ± 0.007	1.570 ± 0.08	0.677 ± 0.04	4.017 ± 1.72	0.295 ± 0.51	0.0253 ± 0.007	0.0012 ± 0.0004	16.193 ± 1.97
Ac-CG	63.185 ± 0.23	26.281 ± 0.23	3.571 ± 0.10	2.424 ± 0.08	1.179 ± 0.03	0.147 ± 0.004	0.775 ± 0.006	0.716 ± 0.04	4.545 ± 1.69	0.082 ± 0.37	0.0268 ± 0.004	0.0010 ± 0.0005	15.609 ± 1.83
Ne-CG	62.820 ± 0.24	26.336 ± 0.22	3.492 ± 0.09	2.402 ± 0.08	1.307 ± 0.04	0.177 ± 0.003	0.605 ± 0.004	0.744 ± 0.05	5.590 ± 1.68	0.094 ± 0.56	0.0283 ± 0.003	0.0015 ± 0.0002	13.665 ± 1.77
Al-CG	62.826 ± 0.24	26.534 ± 0.22	3.598 ± 0.10	2.212 ± 0.07	1.628 ± 0.03	0.149 ± 0.004	0.569 ± 0.005	0.749 ± 0.04	9.497 ± 1.63	1.515 ± 0.47	0.0160 ± 0.002	0.0074 ± 0.0002	5.628 ± 1.46

Note: S_{BET}, BET surface area; $A_{t\text{-}Plot}$, t-Plot micropore area; V_{meso}, BJH desorption cumulative volume of pores; $V_{t\text{-}Plot}$, t-Plot micropore volume; and D_{avr}, BJH desorption average pore diameter.

3.1.3. FTIR Analysis

The FTIR spectra of RCG and the modified coal gangues are shown in Figure 1b. According to the different wavenumber ranges of different functional groups, the functional groups of coal gangue samples were detected, and the vibration bands were very different from each other. For the RCG, the peaks at 3698, 3654, and 3621 cm^{-1} were the stretching vibration peaks that were attributed to the -OH bonds [48], which were generated from the inner and outer-hydroxyl stretching vibrations of kaolinite. The broad peak at 3443 cm^{-1} was associated with -OH bond stretching vibration absorption, and the band at 1625 cm^{-1} may be due to H-O-H bending vibrations from physisorbed water [49,50]. The peaks at 1033 cm^{-1} and 1006 cm^{-1} referred to Si-O-Si stretching vibration, the peaks at around 798 cm^{-1} and 695 cm^{-1} were attributed to Si-O bond symmetric stretching vibration, and the bands at 470 cm^{-1} were attributed to the stretching vibration of Si-O-Si [51]. In addition, the peaks at 912 cm^{-1} and 537 cm^{-1} referred to Al-OH bending vibration and stretching vibration in the octahedral aluminum structure, respectively.

In comparison with RCG, the intensity of the absorption peak of the modified gangue was weakened, indicating that structural water reduced. For Ac-CG and Ne-CG, the absorption peaks at 3698, 3654, and 3621 cm^{-1} disappeared and the Si-O-Al absorption peaks at 695 and 537 cm^{-1} were weakened, which indicated that kaolinite was conversed to metakaolinite [52], while for Al-CG, the intensity of the absorption peaks diminished, and two bands at 1033 and 1006 cm^{-1} disappeared, which was related to the depolymerization and collapse of the silica tetrahedral structure. The band of Al-CG at 464 cm^{-1} was the bending vibration mode of Si-O-Al [53], and a new absorption peak at 1089 cm^{-1} indicated the formation of a new phase [54], which might be caused by the asymmetric stretching vibration of Si-O-Si in the C-S-H gels.

3.1.4. SEM Analysis

The SEM images of RCG and modified coal gangue samples are presented in Figure 2. It can be seen that RCG had an irregular lamellar structure and a rough surface, which

might be associated with the flaky structure of kaolinite (Figure 2a). As observed, the kaolinite microstructure obviously changes with the calcium-modified coal gangue (in Figure 2b–d), indicating that its original structure was destructed and active reaction sites were increased [35]. In Figure 2b,c, the surfaces of Ac-CG and Ne-CG became dense and smooth, which was associated with the transformation of kaolinite to metakaolinite at high temperatures; they did not further react with Ca^{2+} under acidic and neutral solutions. When the coal gangue was modified with alkali situation (in Figure 2d), the surface structure became complicated and clusters (C-S-H gels) occurred on the surface of Al-CG; thus, the potential gelation activity was improved [55]. Additionally, some small needle-shaped crystals (AFt) could be detected in the pores, and the results were consistent with the results of Mola Abasi et al. [56] and Han et al. [57], which make the surface structure more complicated; thus, the adsorption process was facilitated. The SEM images were consistent with the XRD results.

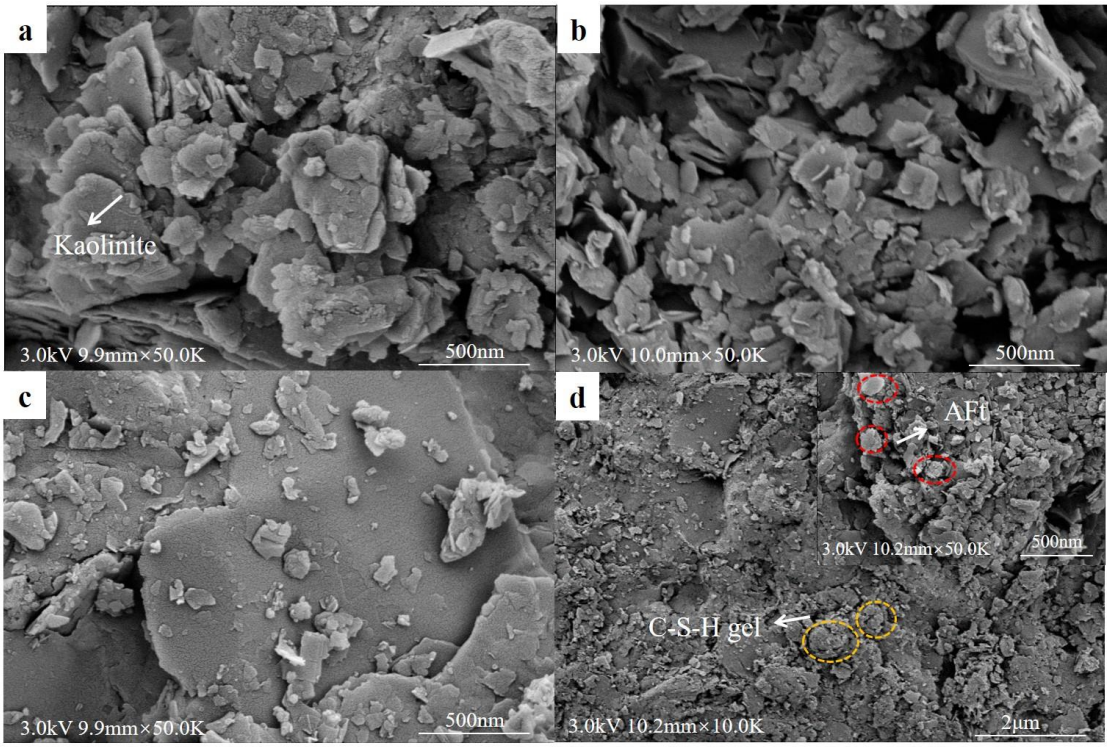

Figure 2. SEM images of different samples ((**a**): RCG, (**b**): Ac-MCG, (**c**): Ne-LCG, and (**d**): Al-CG).

3.1.5. BET Analysis

The textural characteristic of RCG and modified coal gangue samples are shown in Table 1. The results of BET analysis indicated that Al-CG had larger specific surface area (9.497 $m^2\ g^{-1}$), smaller pore size (5.628 nm), larger micropore area (1.515 $m^2\ g^{-1}$), and bigger volume (0.0074 $cm^2\ g^{-1}$) than other samples. This was attributed to the more complex surface structure of Al-CG, which was associated with the generation of needle-like crystals (AFt) and C-S-H gels under alkaline modification conditions. The enlarged specific surface area would provide coal gangue with more adsorption sites, thereby increasing its physical adsorption capacity.

3.2. Phosphate Adsorption of Raw and Calcium-Modified Coal Gangues

3.2.1. Adsorption Kinetics of Phosphate

The adsorption kinetics based on the pseudo first-order and pseudo second-order model are shown in Figure 3, and the fitting parameters are listed in Table 2. According to Table 2, it can be seen that the experimental data of the pseudo-second-order model fit better than the pseudo-first-order model, indicating that the pseudo-second-order model provides

good fitness between the experimental values and the model. In the pseudo-second-order model, the R^2 of modified gangue is higher than that of RCG, which indicates that the fitting effect of RCG is poor and the fitting effect of activated gangue is better. It can be seen from Table 2 that the fitting R^2 of the pseudo second-order model for Al-CG is the highest (R^2 = 0.946), showing the largest equilibrium adsorption capacity, which indicates that the pseudo second-order model can better describe the phosphate adsorption process. The value calculated with this model was 2.283 mg g^{-1}, which was 16.42, 6.39 and 3.43 times higher than that of RCG, Ac-CG, and Ne-CG, respectively.

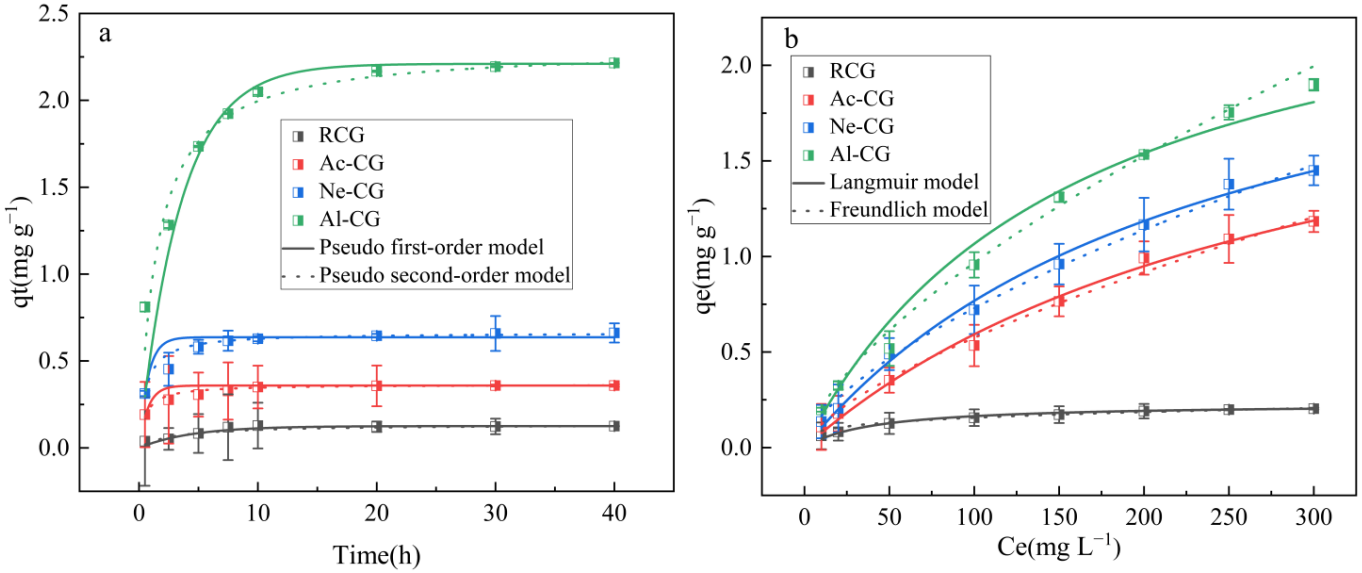

Figure 3. Adsorption kinetics curves (**a**) and adsorption isotherms curves (**b**) of coal gangue samples toward phosphate. Error bars represent standard error of the mean (*n* = 3).

Table 2. Parameters of phosphate adsorption kinetic and isotherm of coal gangue samples.

Sample ID	Pseudo First-Order Model			Pseudo Second-Order Model			Langmuir Model				Freundlish Model		
	k_1 (h^{-1})	q_e ($mg \cdot g^{-1}$)	R^2	k_2 ($g \cdot mg^{-1} \cdot h^{-1}$)	q_e ($mg \cdot g^{-1}$)	R^2	K_l ($L \cdot mg^{-1}$)	q_m ($mg \cdot g^{-1}$)	R^2	n	K_f $[mg^{(1-n)}L^n g^{-1}]^{-1}$	R^2
RCG	0.267	0.126	0.878	2.910	0.139	0.845	0.029	0.221	0.980	1.019	0.033	0.981
Ac-CG	1.524	0.336	0.732	5.457	0.357	0.939	0.003	2.510	0.992	1.008	0.023	0.992
Ne-CG	0.845	0.625	0.750	2.094	0.665	0.935	0.004	2.734	0.994	1.006	0.035	0.994
Al-CG	0.400	2.129	0.856	0.311	2.283	0.946	0.004	3.599	0.995	1.005	0.045	0.994

3.2.2. Adsorption Isotherms of Phosphate

The adsorption isotherm based on the Langmuir and Freundlich models were shown in Figure 3, and the fitting parameters were listed in Table 2. Based on R^2 values, it can be seen that the adsorption for all samples fit better with the Langmuir model than the Freundlich model, and the calcium-modified coal gangues showed better phosphate adsorption capacity than RCG. According to the fitting results of the Langmuir model, the maximum theoretical adsorption capacity of the available phosphorus of Al-CG was the highest (3.599 mg g^{-1}), which was approximately 16.29, 1.43, and 1.32 times higher than that of the RCG, Ac-CG, and Ne-CG samples, respectively.

3.3. Phosphate Desorption of Raw and Calcium-Modified Coal Gangues

The desorption curves of the RCG and modified samples desorbed by distilled water and $NaHCO_3$ solutions are shown in Figures 4 and 5, respectively. Among them, the gangues used in Figure 4 were the samples after phosphate adsorption in the adsorption isotherm experiment, while the gangues in Figure 5 were the samples after 40 h of phosphate adsorption in the adsorption kinetics experiment.

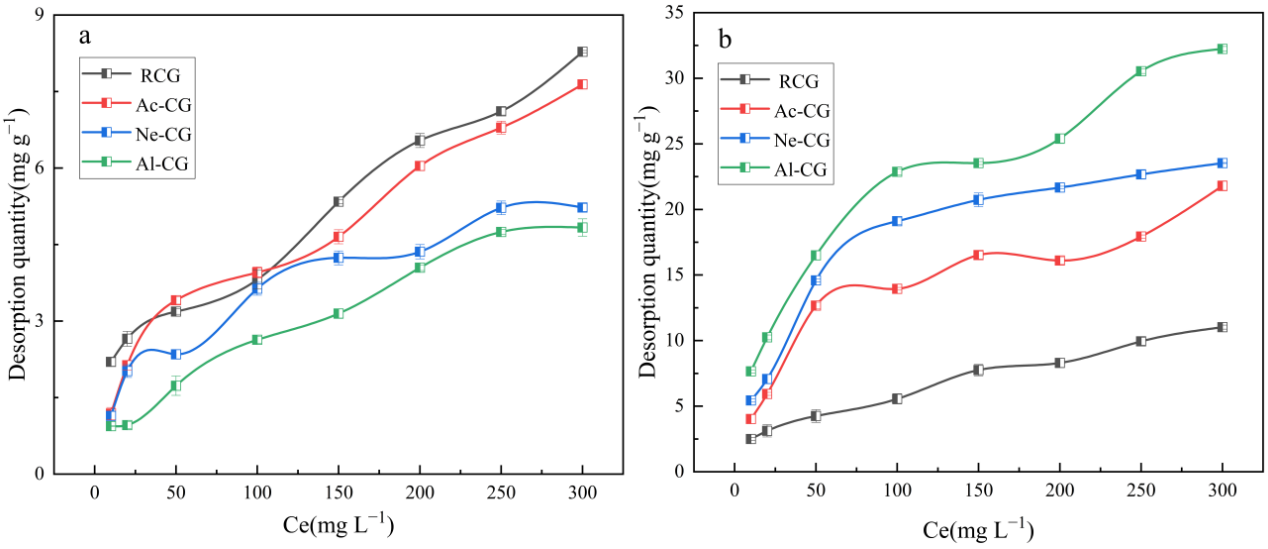

Figure 4. Desorption curves of coal gangue samples toward phosphate for 10h; the desorbents are distilled water (**a**) and $NaHCO_3$ solution (**b**), respectively, and the coal gangue samples are those that have absorbed phosphate in the adsorption isotherms experiment. Error bars represent standard error of the mean (n = 3).

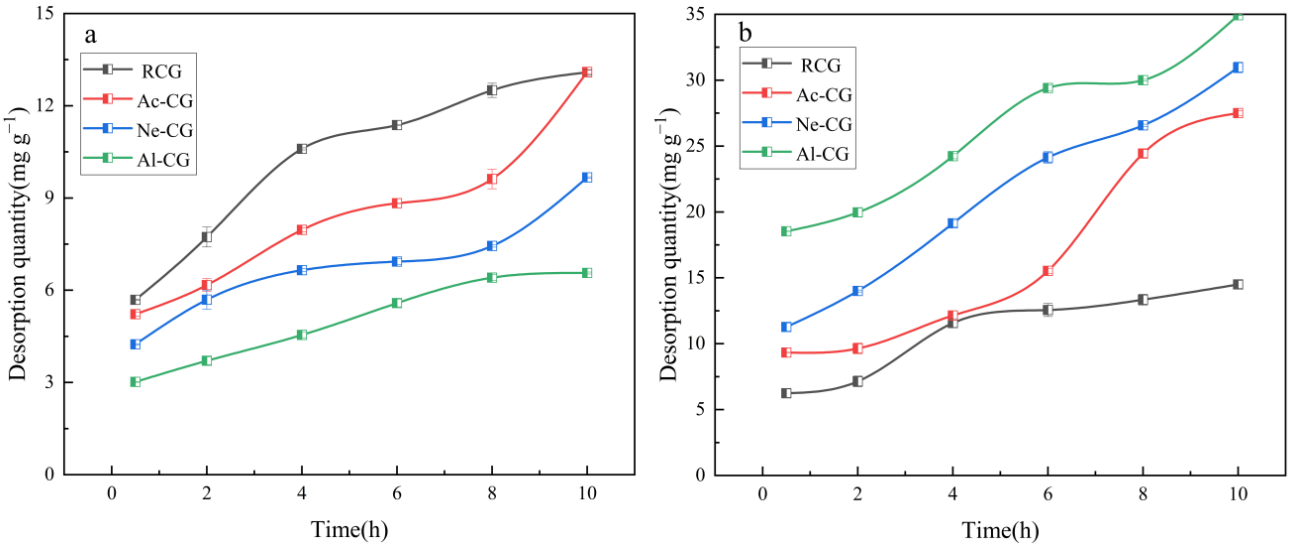

Figure 5. Desorption curves of coal gangue samples toward phosphate under different times; the desorbents are distilled water (**a**) and $NaHCO_3$ solution (**b**) respectively, and the coal gangue samples are those that have absorbed phosphate for 40 h in the adsorption kinetics experiment. Error bars represent standard error of the mean (n = 3).

It can be seen from Figure 4 that the desorption curve of distilled water was obviously different than that of $NaHCO_3$ for modified coal gangues, while those two curves changed little for RCG. Moreover, compared with other samples, the phosphate concentration was the smallest when the Al-CG was desorbed by distilled water, and the phosphate concentration was the largest when the Al-CG was desorbed by $NaHCO_3$. For example, at the concentration of 300 mg/L, the filtrate concentration was 8.280 mg/L for RCG and 4.833 mg/L for Al-CG when distilled water was used as the desorbent, while the filtrate concentration was 11.027 mg/L for RCG and 32.240 mg/L for Al-CG when the $NaHCO_3$ solution was used as the desorbent.

Furthermore, it can be seen from Figure 5 that phosphate concentrations of filtrate gradually increased, and the concentration desorbed by $NaHCO_3$ solution was higher than that desorbed by H_2O, namely, when Al-CG was desorbed by distilled water, the phosphate concentration of filtrate was the smallest, which was lower than that of other coal gangues, while when Al-CG was desorbed by $NaHCO_3$, the phosphate concentration of the filtrate was the largest. For example, at a desorption time of 10 h, the filtrate concentration was 13.090 mg/L for RCG and 6.560 mg/L for Al-CG when distilled water was used as the desorbent, while the filtrate concentration was 14.500 mg/L for RCG and 34.933 mg/L for Al-CG when $NaHCO_3$ solution was used as the desorbent.

4. Discussion

4.1. Analysis of Phosphate Adsorption Mechanism by Calcium-Modified Coal Gangue

It is reported that new phases were generated; the kaolinite and illite disappeared in coal gangue after the grinding and high-temperature calcination; and the Al-O, Si-O-Si, and Si-O bonds in coal gangue broke, producing an expansion in crystal spacing and an increase in activity of SiO_2 and Al_2O_3 [42,58–61]. In this study, we found that when stimulating the calcined coal gangue with alkaline Ca^{2+} solution, Ca^{2+} would react with the amorphous SiO_2 of coal gangue to generate C-S-H gel (Equation (5)) and reacted with $SO_4{}^{2-}$ and $[Al(OH)_6]^{3-}$ to form AFt (Equation (6)).

$$4Ca(OH)_2 + 6SiO_2 \rightarrow Ca_4Si_6O_{14}(OH)_4 \cdot 2H_2O \quad (5)$$

$$2[Al(OH)_6]^{3-} + 6Ca^{2+} + 3SO_4^{2-} + 26H_2O \rightarrow Ca_6Al_2(SO_4)_3(OH)_{12} \cdot 26H_2O \quad (6)$$

C-S-H and AFt benefited the improving of the adsorption capacity of coal gangue toward phosphate, which was because Ca^{2+} and Al^{3+} could be dissociated from C-S-H gels and AFt in KH_2PO_4 solution (pH = 6), with the corresponding chemical equations as follows:

$$Ca_4Si_6O_{14}(OH)_4 \cdot 2H_2O + 8H^+ \rightarrow 4Ca^{2+} + 6H_2SiO_3 + 2H_2O \quad (7)$$

$$Ca_6Al_2(SO_4)_3(OH)_{12} \cdot 26H_2O \rightarrow 2[Al(OH)_6]^{3-} + 6Ca^{2+} + 3SO_4^{2-} + 26H_2O \quad (8)$$

$$[Al(OH)_6]^{3-} + 6H^+ \rightarrow Al^{3+} + 6H_2O \quad (9)$$

The adsorption mechanism of Al-CG toward phosphate was related to four processes: physical adsorption, electrostatic adsorption, ion exchange, and chemical precipitation, which can be seen in Figure 6. (i) The internal structures of Al-CG were more complex after the modified process [62], and then its physical adsorption capacity toward ions improved. (ii) The negatively charged phosphates were adsorbed by free Ca^{2+} and Al^{3+} through electrostatic adsorption. (iii) AFt provides more -OH, and its presence could participate in phosphate adsorption reactions through ion exchange [63]. (iv) The chemical reaction between Ca^{2+}, OH-, and phosphate forms $Ca_5(PO_4)_3OH$ precipitates, and Ca^{2+} and Al^{3+} react with phosphate to form Ca-P and Al-P precipitates, which are attached to the surface of gangue. The reaction equations are as follows:

$$5Ca^{2+} + 7OH^- + 3H_2PO_4{}^- \rightarrow Ca_5(PO_4)_3OH \downarrow + 6H_2O \quad (10)$$

$$Ca^{2+} + 2H_2PO_4^- \rightarrow Ca - P \downarrow \quad (11)$$

$$Al^{3+} + 3H_2PO_4^- \rightarrow Al - P \downarrow \quad (12)$$

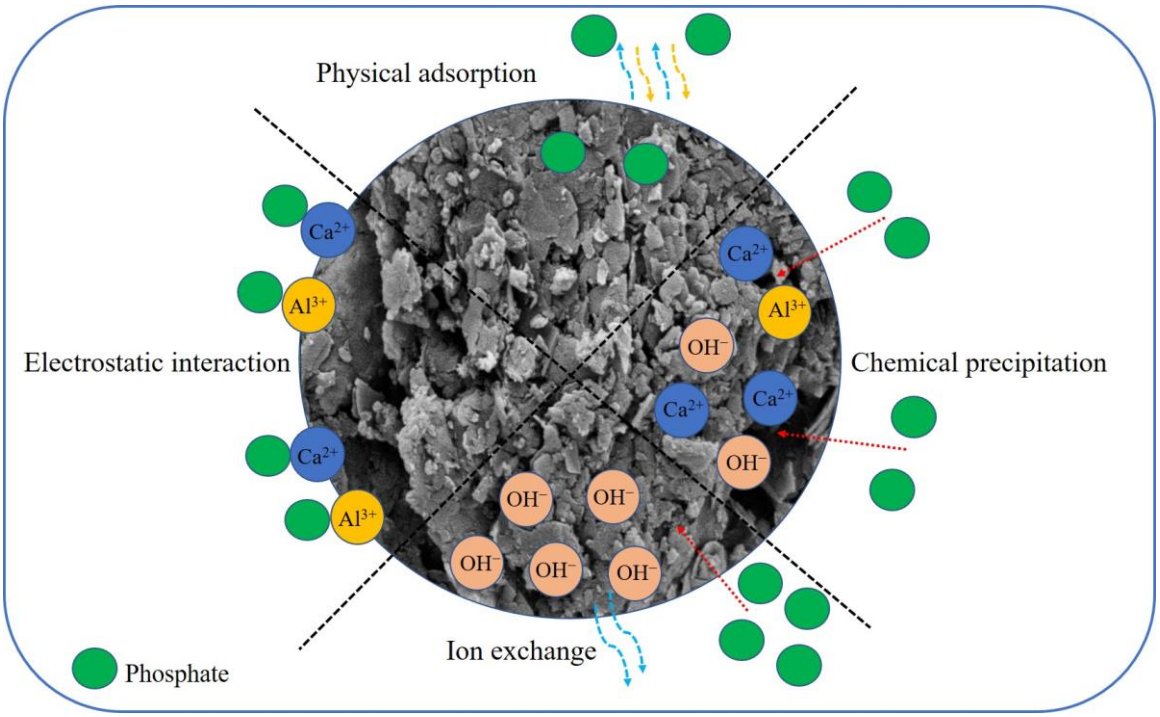

Figure 6. The mechanisms of phosphate adsorption of Al-CG.

4.2. Enlightenment of Modified Coal Gangue on Phosphate Retention and Release Capacity

The adsorption experiments indicated that RCG had limited adsorption capacity toward phosphate, and the maximum adsorption capacity simulated by Langmuir isotherm model was just 0.221 mg g^{-1}. However, the adsorption capacity of modified coal gangues improved largely through calcium-modification; the maximum adsorption capacity toward phosphate by the Langmuir model of Ac-CG and Ne-CG was 2.510 mg g^{-1} and 2.734 mg g^{-1}, respectively; and the maximum adsorption capacity of Al-CG reached 3.599 mg g^{-1}. The maximum adsorption capacity toward the phosphate of RCG was lower than that of some agricultural soils in the relevant literature, for example, Huang et al. [64] reported that the maximum phosphate adsorption capacity of Cixi paddy soils by Langmuir model is 0.235–0.186 mg g^{-1}, and that of Jinxian paddy soils is 0.44–1.55 mg g^{-1}; Eslamian et al. [65] reported that the maximum phosphate adsorption capacity of sandy is 0.250 mg g^{-1} and the maximum phosphate adsorption capacity of clay loam is 0.222 mg g^{-1}; and Bubbaa et al. [66] reported that the maximum phosphate adsorption capacity of Nymolle sands by Langmuir model is 0.266mg g^{-1}. Thus, we believe that using RCG as filling material to replace soil substrates might accelerate nutrient loss and lead to the eutrophication of water bodies in the coal mining area. The maximum phosphate adsorption capacity of Ac-CG and Ne-CG was higher than that of the agricultural soils mentioned above but lower than that of some biochars. For example, the maximum phosphorus adsorption capacity of rice husk biochar is 2.91 mg g^{-1}, and the maximum phosphorus adsorption capacity of lanthanum modified biochar is 2.836 mg g^{-1} [67], while Al-CG had comparable phosphate adsorption capacity with the biochars, indicating that it can be used as a favorable soil conditioner. Moreover, Al-CG also had perfect desorption characteristics toward phosphate, when we used distilled water to desorb the Al-CG sample that had absorbed phosphate, the phosphate concentrations of filtrate were lower than that of other samples, while when it was desorbed with $NaHCO_3$ solution, the phosphate concentrations were higher than other samples. It is indicated that the phosphate adsorbed by Al-CG could be held longer and released slowly, which is benefit of the long-term effectiveness of phosphorus for plant.

4.3. Application Advantages and Directions of Modified Coal Gangue

In this study, we explored the adsorption and desorption characteristics of calcium-modified coal gangues toward available phosphorus, and we believe that the Al-CG has some application advantages, including inexpensive, eco-friendly, and durable application. (i) Inexpensive: coal gangue is a common solid waste with a large number of emissions, the modified process of coal gangue is simple, and the energy consumption is low; thus, the production cost of Al-CG is relatively inexpensive. (ii) Eco-friendly: the use of coal gangue as a filling material would lead to the rapid loss of soil nutrients and cause the eutrophication of water bodies in coal mining area. However, after modification, the structure of coal gangue was changed and new substances were produced, which were conducive to the reclaimed soil nutrient sequestration and the control of water bodies eutrophication. (iii) Durable application: after the modification of alkali situation, C-S-H gel and AFt were generated, which made the structure of modified coal gangue more stable and chemically resistant, and the applicated life was increased.

All in all, Al-CG had preferable phosphate adsorption and desorption capacity, and its ecological and economic benefits were better than RCG. We proposed that Al-CG had perfect adsorption capacity toward phosphate, which could be used as an adsorbent to remove phosphate in water bodies in the environmental field. It could also maintain the effectiveness of phosphate, which could also be used as a soil conditioner to enhance soil available phosphorus content in agriculture field. Moreover, it could be used as a better filling material to improve reclaimed soil quality in the coal mining area.

5. Conclusions

In this study, we prepared three calcium-modified coal gangues (Ac-CG, Ne-CG, and Al-CG). We mainly investigated the phosphate adsorption and desorption characteristics of raw and modified coal gangues and explored the phosphate adsorption and desorption mechanisms of modified coal gangues. The main findings of this study are summarized as follows.

1. Al-CG had better adsorption and desorption effects, and the adsorption process was more in line with the pseudo second-order model and the Langmuir isotherm adsorption model, where the Langmuir maximum adsorption capacity of Al-CG was the highest (3.599 mg g^{-1}).
2. The better adsorption effect of Al-CG was contributed to the generation of C-S-H and AFt, which provided a larger specific surface area (9.497 m^2 g^{-1}) and more Ca^{2+}, Al^{3+}, and hydroxyl groups.
3. When the Al-CG sample that absorbed phosphate was desorbed by distilled water, the desorption amount of phosphate was the lowest, and when using $NaHCO_3$ solution (pH = 8.5) to desorb it, the desorption amount was highest.
4. The study demonstrated that calcium modification with alkali condition was an effective way to realize the resource utilization of coal gangue, which can be used as a filling material in the reclamation area, as a soil conditioner in agricultural production, and as a phosphorus removal agent in water bodies.

Author Contributions: Conceptualization, T.Y. and X.M.; methodology, X.M. and X.L.; formal analysis and investigation, T.Y., X.J., M.S. and X.M.; writing—original draft preparation, T.Y. and X.M.; writing—review and editing, T.Y., X.J., M.S. and X.M.; funding acquisition, X.M. and X.L.; resources: X.M. and X.L.; and supervision, X.M. and X.L. All authors have read and agreed to the published version of the manuscript.

Funding: This research was funded by the National Natural Science Foundation of China (Grant No. 41907399 and 42077446).

Institutional Review Board Statement: This study does not require ethical approval, so this statement is excluded.

Informed Consent Statement: Informed consent was obtained from all subjects involved in the study.

Data Availability Statement: The data provided in this study can be obtained at the request of the corresponding author.

Acknowledgments: The authors would like to thank the editor and anonymous reviewers for their valuable suggestions, which help to improve the quality of the paper greatly. This work was supported by the National Natural Science Foundation of China (Grant No. 41907399 and 42077446). The authors gratefully acknowledge test support from National Engineering Research Center for the Efficient Utilization of Soil and Fertilizer Resources of Shandong Agricultural University (Taian).

Conflicts of Interest: The authors declare no conflict of interest.

References

1. Li, J.Y.; Wang, J.M. Comprehensive utilization and environmental risks of coal gangue: A review. *J. Clean. Prod.* **2019**, *239*, 117946. [CrossRef]
2. Zhang, W.Q.; Dong, C.W.; Huang, P.; Sun, Q.; Li, M.; Chai, J. Experimental Study on the Characteristics of Activated Coal Gangue and Coal Gangue-Based Geopolymer. *Energies* **2020**, *13*, 2504. [CrossRef]
3. Romero, M.; Padilla, I.; Contreras, M.; López-Delgado, A. Mullite-Based Ceramics from Mining Waste: A Review. *Mineral* **2021**, *11*, 332. [CrossRef]
4. Alfarzaeai, M.S.; Niu, Q.; Zhao, J.Q.; Eshaq, R.M.A.; Hu, E. Coal/Gangue Recognition Using Convolutional Neural Networks and Thermal Images. *IEEE Access* **2020**, *8*, 76780–76789. [CrossRef]
5. Querol, X.; Zhuang, X.; Font, O.; Izquierdo, M.; Alastuey, A.; Castro, I.; van Drooge, B.L.; Moreno, T.; Grimalt, J.O.; Elvira, J.; et al. Influence of soil cover on reducing the environmental impact of spontaneous coal combustion in coal waste gobs: A review and new experimental data. *Int. J. Coal Geol.* **2011**, *85*, 2–22. [CrossRef]
6. Song, L.; Liu, S.J.; Li, W.W. Quantitative inversion of fixed carbon content in coal gangue by thermal infrared spectral data. *Energies* **2019**, *12*, 1659. [CrossRef]
7. Huang, Y.L.; Zhang, J.X.; Yin, W.; Sun, Q. Analysis of overlying strata movement and behaviors in caving and solid backfilling mixed coal mining. *Energies* **2017**, *10*, 1057. [CrossRef]
8. Bi, H.B.; Wang, C.X.; Lin, Q.Z.; Jiang, X.D.; Jiang, C.L.; Bao, L. Pyrolysis characteristics, artificial neural network modeling and environmental impact of coal gangue and biomass by TG-FTIR. *Sci. Total Environ.* **2021**, *751*, 142293. [CrossRef]
9. Wang, J.M.; Li, X.F.; Bai, Z.K.; Huang, L.B. The effects of coal gangue and fly ash on the hydraulic properties and water content distribution in reconstructed soil profiles of coal-mined land with a high groundwater table. *Hydrol. Process.* **2016**, *31*, 687–697. [CrossRef]
10. Zhang, Y.L.; Ling, T.C. Reactivity activation of waste coal gangue and its impact on the properties of cement-based materials—A review. *Constr. Build. Mater.* **2020**, *234*, 117424. [CrossRef]
11. Stracher, G.B.; Taylor, T.P. Coal fires burning out of control around the world: Thermodynamic recipe for environmental catastrophe. *Int. J. Coal Geol.* **2004**, *59*, 7–17. [CrossRef]
12. Nathan, Y.; Dvorachek, M.; Pelly, I.; Mimran, I. Characterization of coal fly ash from Israel. *Fuel* **1999**, *78*, 205–213. [CrossRef]
13. Shepley, M.G.; Pearson, A.D.; Smith, G.D.; Banton, C.J. The impacts of coal mining subsidence on groundwater resources management of the East Midlands Permo-Triassic Sandstone aquifer, England. *Q. J. Eng. Geol. Hydrogeol.* **2008**, *41*, 425–438. [CrossRef]
14. Rahnema, H.; Mirasi, S. Seismic and geotechnical study of land subsidence and vulnerability of rural buildings. *Int. J. Geosci.* **2012**, *3*, 878–884. [CrossRef]
15. Hejmanowski, R. Modeling of time dependent subsidence for coal and ore deposits. *Int. J. Coal Sci. Technol.* **2015**, *2*, 287–292. [CrossRef]
16. Akbar, G.; Ali, M.; Homayon, S.; Mahasa, R. Effects of groundwater withdrawal on land subsidence in Kashan Plain, Iran. *Bull. Eng. Geol. Environ.* **2016**, *75*, 1157–1168.
17. Pone, J.D.N.; Hein, K.A.A.; Stracher, G.B.; Annegarn, H.J.; Finkleman, R.B.; Blake, D.R.; McCormack, J.K.; Schroeder, P. The spontaneous combustion of coal and its by-products in the Witbank and Sasolburg coalfields of South Africa. *Int. J. Coal Geol.* **2007**, *72*, 124–140. [CrossRef]
18. Zheng, L.P.; Zhu, L.; Wang, W.; Guo, L.; Chen, B.B. Land subsidence related to coal mining in China revealed by L-Band InSAR analysis evaluation methods. *Int. J. Environ. Res. Public Health* **2020**, *17*, 1170. [CrossRef]
19. Xu, X.H.; Lao, X.B.; Wu, J.F.; Zhang, Y.X.; Xu, X.Y.; Li, K. Microstructural evolution, phase transformation, and variations in physical properties of coal series kaolin powder compact during firing. *Appl. Clay Sci.* **2015**, *115*, 76–86. [CrossRef]
20. Polak, K.; Różkowski, K.; Czaja, P. Causes and Effects of Uncontrolled Water Inrush into a Decommissioned Mine Shaft. *Mine Water Environ.* **2015**, *35*, 128–135. [CrossRef]
21. Chen, B.; Zhang, Y.M.; Chen, Q.; Yang, F.; Liu, X.P.; Wu, J.G.; Wang, P.M. Effect of mineral composition and w/c ratios to the growth of AFt during cement hydration by In-Situ powder X-ray diffraction analysis. *Materials* **2020**, *13*, 4963. [CrossRef] [PubMed]
22. Tang, Q.; Li, L.Y.; Zhang, S.; Zheng, L.G.; Miao, C.H. Characterization of heavy metals in coal gangue-reclaimed soils from a coal mining area. *J. Geochem. Explor.* **2018**, *186*, 1–11. [CrossRef]

23. Kumar, D.; Singh, B. The use of coal fly ash in sodic soil reclamation. *Land. Degrad. Dev.* **2003**, *14*, 285–299. [CrossRef]
24. Cheng, W.; Bian, Z.F.; Dong, J.H.; Lei, S.G. Soil properties in reclaimed farmland by filling subsidence basin due to underground coal mining with mineral wastes in China. *Trans. Nonferrous Met. Soc. China* **2014**, *24*, 2627–2635. [CrossRef]
25. Guo, Y.X.; Yan, K.Z.; Cui, L.; Cheng, F.Q. Improved extraction of alumina from coal gangue by surface mechanically grinding modification. *Powder Technol.* **2016**, *302*, 33–41. [CrossRef]
26. Wang, S.B.; Luo, K.L.; Wang, X.; Sun, Y.Z. Estimate of sulfur, arsenic, mercury, fluorine emissions due to spontaneous combustion of coal gangue an important part of Chinese emission inventories. *Environ. Pollut.* **2016**, *209*, 107–113. [CrossRef]
27. Li, Y.; Yao, Y.; Liu, X.M.; Sun, H.H.; Ni, W. Improvement on pozzolanic reactivity of coal gangue by integrated thermal and chemical activation. *Fuel* **2013**, *109*, 527–533. [CrossRef]
28. Motasemi, F.; Afzal, M.T. A review on the microwave-assisted pyrolysis technique. *Renew. Sust. Energ. Rev.* **2013**, *28*, 317–330. [CrossRef]
29. Aglietti, E.F.; Lopez, J.M.P.; Pereira, E. Mechanochemical effects in kaolinite grinding. I. Textural and physicochemical aspects. *Int. J. Miner. Process.* **1986**, *16*, 125–133. [CrossRef]
30. Suraj, G.; Iyer, C.S.P.; Rugmini, S.; Lalithambika, M. The effect of micronization on kaolinites and their sorption behaviour. *Appl. Clay Sci.* **1997**, *12*, 111–130. [CrossRef]
31. Boldyreva, E. Mechanochemistry of inorganic and organic systems: What is similar, what is different? *Chem. Soc. Rev.* **2013**, *42*, 7719–7738. [CrossRef] [PubMed]
32. Jaesuk, R. Improvement on reactivity of cementitious waste materials by mechano-chemical activation. *Mater. Lett.* **2003**, *58*, 903–906.
33. Yang, N.R. Processes and effects of mechanochemistry(II)—Processes and application of mechanochemistry. *J. Build. Mater.* **2000**, *3*, 93–97. (In Chinese)
34. Stellacci, P.; Liberti, L.; Notarnicola, M.; Bishop, P.L. Valorization of coal fly ash by mechano-chemical activation: Part II. Enhancing pozzolanic reactivity. *Chem. Eng. J.* **2009**, *149*, 19–24. [CrossRef]
35. Li, C.; Wan, J.H.; Sun, H.H.; Li, L.T. Investigation on the activation of coal gangue by a new compound method. *J. Hazard. Mater.* **2010**, *179*, 515–520. [CrossRef] [PubMed]
36. Zhou, C.; Liu, G.; Yan, Z.; Fang, T. Transformation behavior of mineral composition and trace elements during coal gangue combustion. *Fuel* **2012**, *97*, 644–650. [CrossRef]
37. Guo, W.; Li, D.X.; Chen, J.H.; Yang, N.R. Structure and pozzolanic activity of calcined coal gangue during the process of mechanical activation. *J. Wuhan Univ. Technol.* **2009**, *24*, 326–329. [CrossRef]
38. Liu, F.Q.; Xie, M.Z.; Yu, G.Q.; Ke, C.Y.; Zhao, H.L. Study on Calcination Catalysis and the Desilication Mechanism for Coal Gangue. *ACS Sustain. Chem. Eng.* **2021**, *9*, 10318–10325. [CrossRef]
39. Han, J.Y.; Song, X.Y.; Gao, Z.H. Excitation effect of soluble glass on composite system with calcined coal gangue and slag. *Appl. Mech. Mater.* **2012**, *174–177*, 30–34. [CrossRef]
40. Livingston, W.R.; Rogers, D.A.; Chapman, R.J.; Bailey, N.T. The use of coal spoils as feed materials for alumina recovery by acid-leaching. *Hydrometallurgy* **1983**, *10*, 79–96. [CrossRef]
41. Hussain, S.A.; Jamal, R. Evaluation of an HCl process for leaching of low-grade highly siliceous bauxite ore. *Dev. Miner. Process.* **2000**, *13*, 8–14.
42. Zhou, J.M.; Fu, Y.S.; Pan, S.W. The use of modified coal gangue for the remediation and removal of phosphorus in an enclosed water area. *Clean Technol. Environ. Policy* **2021**, *23*, 1327–1339. [CrossRef]
43. Ma, Y.L.; Ma, J.; Peng, H.; Weng, L.P.; Chen, Y.L.; Li, Y.T. Effects of iron, calcium, and organic matter on phosphorus behavior in fluvo-aquic soil: Farmland investigation and aging experiments. *J. Soil Sediment.* **2019**, *19*, 3994–4004. [CrossRef]
44. Gamelas, J.A.F.; Ferra, E.; Rocha, F. An insight into the surface properties of calcined kaolinitic clays: The grinding effect. *Colloid. Surf. A* **2014**, *455*, 49–57. [CrossRef]
45. Frost, R.; Makoens, E.; Kristóf, J.; Kloprogge, T. Modification of kaolinite surfaces through mechanochemical treatment-a mid-IR and near-IR spectroscopic study. *Spectrochim. Acta A* **2002**, *58*, 2849–2859. [CrossRef]
46. Ptáček, P.; Frajkorová, F.; Šoukal, F.; Opravil, T. Kinetics and mechanism of three stages of thermal transformation of kaolinite to metakaolinite. *Powder Technol.* **2014**, *264*, 439–445. [CrossRef]
47. Ye, T.T.; Min, X.Y.; Li, X.J.; Zhang, S.G.; Gao, Y. Improved holding and releasing capacities of coal gangue toward phosphate through alkali-activation. *Chemosphere* **2022**, *287*, 132382. [CrossRef]
48. Bu, N.J.; Liu, X.M.; Song, S.L.; Liu, J.H.; Yang, Q.; Li, R.; Zheng, F.; Yan, L.H.; Zhen, Q.; Zhang, J.F. Synthesis of NaY zeolite from coal gangue and its characterization for lead removal from aqueous solution. *Adv. Powder Technol.* **2020**, *31*, 2699–2710. [CrossRef]
49. Alver, B.E.; Alver, Ö.; Günal, A.; Dikmen, G. Effects of hydrochloric acid treatment on structure characteristics and C2H4 adsorption capacities of Unye bentonite from Turkey: A combined FT-IR, XRD, XRF, TG/DTA and MAS NMR study. *Adsorption* **2016**, *22*, 287–296. [CrossRef]
50. Baccour, A.; Sahnoun, R.D.; Bouaziz, J. Effects of mechanochemical treatment on the properties of kaolin and phosphate–kaolin materials. *Powder Technol.* **2014**, *264*, 477–483. [CrossRef]
51. Ptáček, P.; Kubátová, D.; Havlica, J.; Brandštetr, J.; Šoukal, F.; Opravil, T. The non-isothermal kinetic analysis of the thermal decomposition of kaolinite by thermogravimetric analysis. *Powder Technol.* **2010**, *204*, 222–227. [CrossRef]

52. Mohammadi, R.; Azadmehr, A.; Maghsoudi, A. Enhanced competitive adsorption of zinc and manganese by alginate-iron oxide-combusted coal gangue composite: Synthesizing, characterization and investigation. *J. Environ. Chem. Eng.* **2021**, *9*, 105003. [CrossRef]
53. Li, L.X.; Zhang, Y.M.; Zhang, Y.F.; Sun, J.M.; Hao, Z.F. The thermal activation process of coal gangue selected from Zhungeer in China. *J. Therm. Anal. Calorim.* **2016**, *126*, 1559–1566. [CrossRef]
54. Sun, H.L.; Fen, D.D.; Sun, S.Z.; Zhao, Y.J.; Zhang, L.Y.; Chang, G.Z.; Guo, Q.J.; Wu, J.Q.; Qin, Y.K. Thermal evolution of gas-liquid-solid products and migration regulation of C/H/O elements during biomass pyrolysis. *J. Anal. Appl. Pyrol.* **2021**, *156*, 105128. [CrossRef]
55. Li, Z.F.; Gao, Y.F.; Zhang, J.; Zhang, C.; Chen, J.P.; Liu, C. Effect of particle size and thermal activation on the coal gangue based geopolymer. *Mater. Chem. Phys.* **2021**, *267*, 124657. [CrossRef]
56. MolaAbasi, H.; Semsani, S.N.; Saberian, M.; Khajeh, A.; Li, J.; Harandi, M. Evaluation of the long-term performance of stabilized sandy soil using binary mixtures: A micro- and macro-level approach. *J. Clean. Prod.* **2020**, *267*, 122209. [CrossRef]
57. Han, Y.M.; Xia, J.W.; Chang, H.F.; Xu, J. The influence mechanism of ettringite crystals and microstructure characteristics on the strength of calcium-based stabilized soil. *Materials* **2021**, *14*, 1359. [CrossRef] [PubMed]
58. Wang, B.; Ma, Y.N.; Lee, X.Q.; Wu, P.; Liu, F.; Zhang, X.Y.; Li, L.; Chen, M. Environmental-friendly coal gangue-biochar composites reclaiming phosphate from water as a slow-release fertilizer. *Sci. Total Environ.* **2021**, *758*, 143664. [CrossRef]
59. Qiu, B.B.; Duan, F. Synthesis of industrial solid wastes/biochar composites and their use for adsorption of phosphate: From surface properties to sorption mechanism. *Colloid. Surf. A* **2019**, *571*, 86–93. [CrossRef]
60. Xie, Z.; Xi, Y.; Day, R.; Su, J.; Wu, X. The influence of alkalinity on activation and microstructure of fly ash. *Cem. Concr. Res.* **2001**, *31*, 1245–1249. [CrossRef]
61. Wang, C.L.; Ni, W.; Zhang, S.Q.; Wang, S.; Gai, G.S.; Wang, W.K. Preparation and properties of autoclaved aerated concrete using coal gangue and iron ore tailings. Construction and Building. *Materials* **2016**, *104*, 109–115.
62. Qiu, R.F.; Cheng, F.Q. Modification of waste coal gangue and its application in the removal of Mn^{2+} from aqueous solution. *Water Sci. Technol.* **2016**, *74*, 524–534. [CrossRef] [PubMed]
63. Liu, X.N.; Shen, F.; Smith, R.L., Jr.; Qi, X.H. Black liquor-derived calcium-activated biochar for recovery of phosphate from aqueous solutions. *Bioresour. Technol.* **2019**, *294*, 122198. [CrossRef] [PubMed]
64. Huang, L.M.; Thompson, A.; Zhang, G.L. Long-term paddy cultivation significantly alters topsoil phosphorus transformation and degrades phosphorus sorption capacity. *Soil Till. Res.* **2014**, *142*, 32–41. [CrossRef]
65. Eslamian, F.; Qi, Z.M.; Qian, C. Lime amendments to enhance soil phosphorus adsorption capacity and to reduce phosphate desorption. *Water Air Soil Poll.* **2021**, *232*, 66. [CrossRef]
66. Del Bubba, M.; Arias, C.A.; Brix, H. Phosphorus adsorption maximum of sands for use as media in subsurface flow constructed reed beds as measured by the Langmuir isotherm. *Water Res.* **2003**, *37*, 3390–3400. [CrossRef]
67. Zhao, D.; Qiu, S.K.; Li, M.M.; Luo, Y.; Zhang, L.S.; Feng, M.H.; Yuan, M.Y.; Zhang, K.Q.; Wang, F. Modified biochar improves the storage capacity and adsorption affinity of organic phosphorus in soil. *Environ. Res.* **2022**, *205*, 112455. [CrossRef]